4-3-2023

Hydrogen bonding versus halogen bonding: Spectroscopic investigation of gas-phase complexes involving bromide and chloromethanes

Hayden T. Robinson

Christian T. Haakansson

Timothy R. Corkish

Peter D. Watson

Allan J. McKinley

See next page for additional authors

10.1002/cphc.202200733

Robinson, H. T., Haakansson, C. T., Corkish, T. R., Watson, P. D., McKinley, A. J., & Wild, D. A. (2023). Hydrogen bonding versus halogen bonding: Spectroscopic investigation of gas-phase complexes involving bromide and chloromethanes. ChemPhysChem, 24(7), Article e202200733. https://doi.org/10.1002/cphc.202200733

ChemPhysChem

Research Article
doi.org/10.1002/cphc.202200733

Chemistry Europe
European Chemical Societies Publishing

www.chemphyschem.org

Hydrogen Bonding versus Halogen Bonding: Spectroscopic Investigation of Gas-Phase Complexes Involving Bromide and Chloromethanes

Hayden T. Robinson,[a] Christian T. Haakansson,[a] Timothy R. Corkish,[a] Peter D. Watson,[a, b] Allan J. McKinley,[a] and Duncan A. Wild*[a, c]

Hydrogen bonding and halogen bonding are important non-covalent interactions that are known to occur in large molecular systems, such as in proteins and crystal structures. Although these interactions are important on a large scale, studying hydrogen and halogen bonding in small, gas-phase chemical species allows for the binding strengths to be determined and compared at a fundamental level. In this study, anion photoelectron spectra are presented for the gas-phase complexes involving bromide and the four chloromethanes, CH_3Cl, CH_2Cl_2, $CHCl_3$, and CCl_4. The stabilisation energy and electron binding energy associated with each complex are determined experimentally, and the spectra are rationalised by high-level CCSD(T) calculations to determine the non-covalent interactions binding the complexes. These calculations involve nucleophilic bromide and electrophilic bromine interactions with chloromethanes, where the binding motifs, dissociation energies and vertical detachment energies are compared in terms of hydrogen bonding and halogen bonding.

Introduction

Non-covalent interactions play a crucial role in chemistry, having been studied across a broad range of areas such as crystal engineering, catalysis, material design, and molecular biology.[1–8] Unlike covalent bonds which are generally described as a sharing of electrons between nuclei to form an overall attractive interaction,[9] non-covalent interactions are primarily driven by electrostatics, dispersion, polarisation, Pauli repulsion, and charge transfer, each factor of which affects the overall stability of the interaction.[10–13]

Hydrogen bonding is one type of intermolecular interaction that is commonly observed,[14–16] and occurs when an electronegative atom, such as nitrogen, oxygen, or a halogen, interacts non-covalently with a hydrogen atom that is covalently bonded to a second, relatively more electronegative atom.[9,17] While hydrogen bonding interactions between neutral species are typically weak, such as in the case of the hydrogen bonded water dimer complex having a dissociation energy of approximately 13.2 kJ mol^{-1},[18] hydrogen bonding can also occur between charged species, known as charge-assisted hydrogen bonding, and has been shown to significantly increase the strength of the interaction relative to the neutral analogue.[19]

In contrast, halogen bonding[20–23] occurs when a nucleophilic species interacts non-covalently with a halogen atom (X = Cl, Br, I) that is covalently bonded to a relatively electronegative atom or substituent.[24,25] The ability of halogen atoms to partake in these weak interactions is due to a region of low electron density located on the side of the halogen atom opposite the R–X covalent bond, commonly referred to as a σ-hole.[26] A nucleophile will interact with the halogen at an angle of 160–180° to the R–X bond, thus forming a halogen bond.[27,28] Alternatively, an electrophile will interact with the electron-rich equatorial belt of the halogen at an angle of 90–120° to the R–X bond, which is an interaction that is analogous to halogen bonding.[27] This highlights that directionality is an important factor when considering non-covalent interactions.[28,29] The binding strength of a halogen bond is also highly dependent on how readily electron density can be withdrawn from the halogen, an example of which being the halogen bonded HCl···HCN dimer complex having a strength of 2.5 kJ mol^{-1}, increasing to 11.3 kJ mol^{-1} for the halogen bonded HI···HCN complex.[30] Other types of interactions related to halogen bonding include chalcogen bonding,[31–33] and pnicogen bonding,[34–36] which in some cases have been shown to be similar in strength.[37,38] Halogen bonding interactions have been compared to hydrogen bonding previously, often with a focus on crystal structures or neutral gas-phase species.[30,39–42] This study aims to expand these comparisons to hydrogen and

[a] H. T. Robinson, C. T. Haakansson, T. R. Corkish, P. D. Watson, Prof. A. J. McKinley, Dr. D. A. Wild
School of Molecular Sciences,
The University of Western Australia,
Crawley, Western Australia, 6009
E-mail: duncan.wild@uwa.edu.au
[b] P. D. Watson
Department of Chemistry, University of Oxford,
South Parks Road, Oxford, United Kingdom, OX1 3QZ
[c] Dr. D. A. Wild
School of Science, Edith Cowan University,
Joondalup, Western Australia, 6027
E-mail: d.wild@ecu.edu.au

Supporting information for this article is available on the WWW under https://doi.org/10.1002/cphc.202200733

halogen bonding with charged species, and how these interactions differ with respect to their neutral counterparts.

Chloromethanes represent an ideal series of molecular candidates with respect to studying non-covalent interactions, having the inherent ability to form both hydrogen and halogen bonding interactions with a nucleophile or an electrophile. The increasing chlorination of the base methane molecule also allows for any variation in interaction strength to be studied. Furthermore, the chloromethanes are known to exist in trace amounts in the atmosphere,[43,44] the sources of which being both natural and anthropogenic.[43,45,46] The atmospheric lifetime of the chloromethanes are dependent on reactivity with other species such as hydroxyl radicals,[47] or how readily they undergo photodissociation reactions.[48] Bromine also makes an ideal candidate for studying intermolecular interactions, serving as an intermediate in terms of size and electronegativity relative to other halogens such as chlorine and iodine. Similar to the chloromethanes, bromine is known to exist in trace amounts in the atmosphere,[49] which makes studying gas-phase complexes involving bromine and the chloromethanes relevant in an atmospheric chemistry context. Additionally, bromine can act as a nucleophile or electrophile depending on the presence or absence of excess negative charge localisation.

Anion photoelectron spectroscopy is an ideal technique to study the energetics of gas-phase anion-molecule van der Waals complexes. In this technique photons interact with an anion species causing detachment of an electron. Measuring the kinetic energy of the ejected electron gives the electron binding energy (e_{BE}), which can be used to determine the strength of a non-covalent interaction by comparing the binding energy of an anion-molecule complex to that of its respective bare anion.[50–52]

Ab initio or density functional theory calculations represent methods of locating theoretical electronic structures of chemical systems. Such methods allow for the calculation of theoretical interaction energies, for example those that occur between molecule-molecule complexes,[53–57] or ion-molecule complexes,[58–63] based on the geometry of a chemical species. As the geometry and electronic energy of a chemical species are intrinsically dependent on one another, geometric information can be inferred from experimental energetics, making electronic structure calculations a powerful tool in rationalising experimental data. One method of rationalising an anion photoelectron spectrum is to simulate a vertical detachment energy (VDE) for each optimised electronic structure, by calculating the difference in energy between the optimised ground state anion species and its neutral analogue at the anion geometry. The types of non-covalent interactions stabilising an anion-molecule complex can then be determined by comparing the theoretical VDE to the experimental e_{BE}. It is therefore not surprising that anion photoelectron spectroscopy in conjunction with *ab initio* or density functional theory calculations has previously been successful for studying hydrogen and halogen bonding interactions in various anion-molecule complexes.[64–69]

In this study, we present the photoelectron spectra assigned to bromide anion complexes with the chloromethanes. In addition to anion photoelectron spectroscopy, high-level CCSD(T) calculations were used to compare the types of non-covalent interactions that may occur, with a focus on hydrogen and halogen bonding.

Results and Discussion

Photoelectron Spectroscopy

Figure 1 presents the photoelectron spectra of bromide complexed with each of the four chloromethane solvent molecules, namely $Br^-\cdots CH_3Cl$, $Br^-\cdots CH_2Cl_2$, $Br^-\cdots CHCl_3$, and $Br^-\cdots CCl_4$. Additionally, a bare bromide photoelectron spectrum is also presented. The photodetachment peak positions of the five spectra are summarised in Table 1, alongside the peak positions of the $Br^-\cdots CH_4$ complex which have previously been reported.[70] The defining feature shared among the spectra of the bromide complexes is that they all contain two peaks, each with distinct spin-orbit splitting that is relatively unchanged compared to the bare bromide spectrum. This feature is evidence of non-covalent interactions between the bromide anion and the chloromethane solvent molecules, corroborating that photodetachment is localised to the bromide portion of the complexes; the two peaks are therefore indicative of detachment to the $^2P_{3/2}$ and $^2P_{1/2}$ electronic states of atomic bromine. Hence, the electron stabilisation energy (E_{stab}) can be defined as the energy difference between the respective $^2P_{3/2}$ peak positions of the bromide complex and bare bromide. The E_{stab} serves as a measure of the stabilising effect that a solvent molecule has on an anion moiety, thus resulting in perturbed photodetachment peaks relative to the bare nucleophile.[71] The experimental E_{stab} values for each complex have also been included in Table 1.

Immediately it is observed that for each of the spectra, the photodetachment peaks associated with the bromide complexes are narrower than the peaks of bare bromide. This can be explained by equation 1, where the resultant energy spread (dE_e) of a peak is related to the kinetic energies of the detached electrons and ion beam (E_e and E_i respectively), as well as their masses (m_e and m_i).[72] Electrons detached from ions with higher mass will decrease the $\frac{m_e}{m_i}$ term in the equation, and will therefore have reduced spread in energy and thus narrower peaks. This is evident when comparing the $^2P_{1/2}$ peak of Br^- to the $^2P_{3/2}$ peak of $Br^-\cdots CH_3Cl$, which have similar electron kinetic

Table 1. Peak positions and E_{stab} values obtained from experimental photoelectron spectra.

	$^2P_{3/2}$ [eV]	$^2P_{1/2}$ [eV]	E_{stab} [eV]
Br^-	3.36	3.82	–
$Br^-\cdots CH_4$[a]	3.45	3.91	0.09
$Br^-\cdots CH_3Cl$	3.78	4.24	0.42
$Br^-\cdots CH_2Cl_2$	3.95	4.40	0.59
$Br^-\cdots CHCl_3$	4.09	4.51	0.73
$Br^-\cdots CCl_4$	3.84	4.30	0.48

[a] Zheng and co-workers.[70]

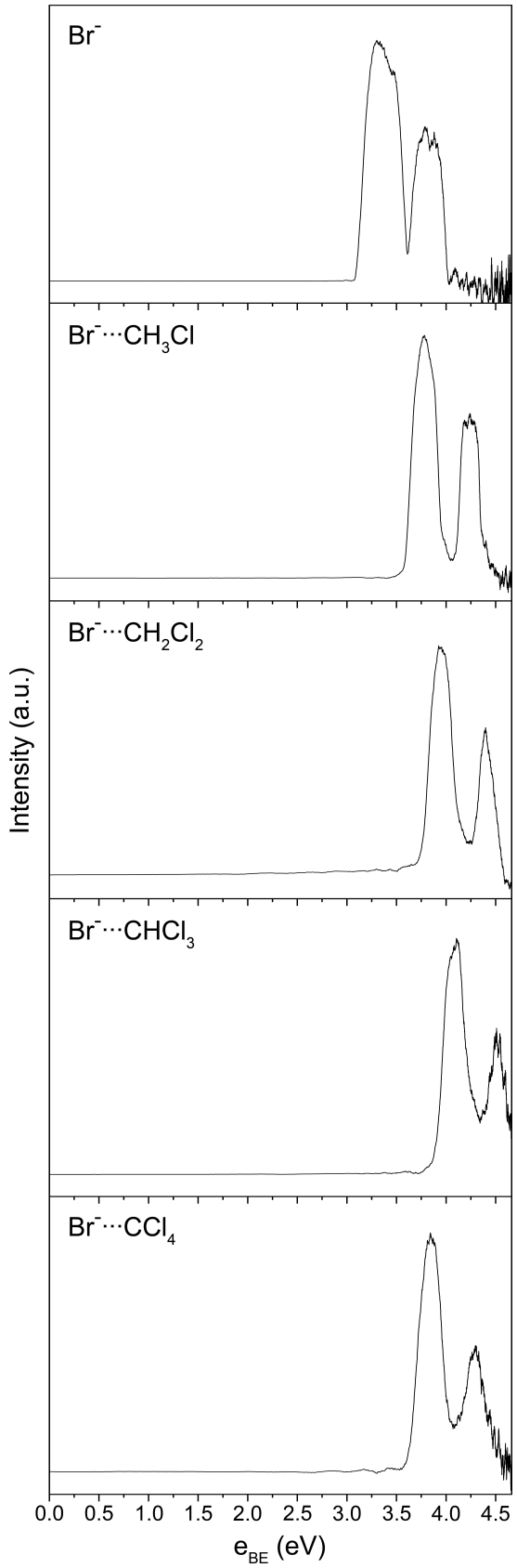

Figure 1. Anion photoelectron spectra of Br^-, $Br^-\cdots CH_3Cl$, $Br^-\cdots CH_2Cl_2$, $Br^-\cdots CHCl_3$ and $Br^-\cdots CCl_4$, produced utilising 4.66 eV laser radiation.

energies of 0.84 eV and 0.88 eV respectively after absorption of 4.66 eV laser radiation, and have the same ion kinetic energy of 1500 eV, but differ noticeably in peak width.

$$dE_e = 4\sqrt{\frac{m_e}{m_i}E_eE_i} \quad (1)$$

Regarding the photoelectron spectrum of $Br^-\cdots CH_3Cl$, the $^2P_{3/2}$ and $^2P_{1/2}$ peaks as reported in Table 1 result in an E_{stab} value of 0.42 eV, indicating a strong interaction between the Br^- nucleophile and the CH_3Cl solvent molecule. For $Br^-\cdots CH_2Cl_2$, photodetachment occurs further upfield than observed for $Br^-\cdots CH_3Cl$, therefore a higher E_{stab} value of 0.59 eV is reported, implying that the non-covalent interactions binding $Br^-\cdots CH_2Cl_2$ are stronger than those binding $Br^-\cdots CH_3Cl$. A similar trend is observed for $Br^-\cdots CHCl_3$, which has the largest E_{stab} value of all the complexes in this study at 0.73 eV, thus indicative of a very tightly bound complex. A sharp decrease in the E_{stab} is reported for $Br^-\cdots CCl_4$, which at 0.48 eV is still a strong interaction, but is less than that seen for $Br^-\cdots CH_2Cl_2$ and $Br^-\cdots CHCl_3$. Accounting for $Br^-\cdots CH_4$,[70] the overall trend observed is that increasing the chlorination of the solvent molecule results in an increase in E_{stab}, which can be explained by the strong electron withdrawing nature of chlorine causing an increasing dipole moment in the order of $CH_4 < CH_3Cl < CH_2Cl_2 < CHCl_3$. This trend ceases at CCl_4 where there is no longer a dipole in the molecule, thus when complexed with Br^- there is a decrease in E_{stab} relative to $Br^-\cdots CHCl_3$. However, it is evident that $Br^-\cdots CCl_4$ is more tightly bound than $Br^-\cdots CH_4$, indicating that the chlorine atoms largely impact the strength of the interaction despite neither CH_4 or CCl_4 having a permanent dipole.

Anion Complexes

Ab initio calculations were employed in order to determine the binding motifs of the bromide chloromethane complexes observed in the photoelectron spectra. Depicted in Figure 2 are structures pertaining to bromide anion interactions with CH_4, CH_3Cl, CH_2Cl_2, $CHCl_3$, and CCl_4 molecules optimised at the CCSD(T)/AVTZ level of theory. All structures shown are minima on the potential energy surface.

One minimum structure was optimised for the $Br^-\cdots CH_4$ complex, which involves the bromide appended to one hydrogen atom in a hydrogen bond (HB) motif. Two minima exist for $Br^-\cdots CH_3Cl$, one of which is an ion-dipole (ID) bound structure where the bromide lies equidistant to the three methyl hydrogens, and the other where the bromide interacts with the chlorine atom in a halogen bond (XB) motif. The $Br^-\cdots CH_2Cl_2$ complex features two minima, one pertaining to a hydrogen bond motif and the other pertaining to a halogen bond motif. Similar structures were optimised for the $Br^-\cdots CHCl_3$ complex, interactions that include hydrogen bonding, halogen bonding, and a third structure where the bromide interacts equidistant to the three chlorine atoms, referred to as an ion-induced dipole (IID) structure. A halogen bond structure and an ion-induced dipole structure were the only two minima optimised

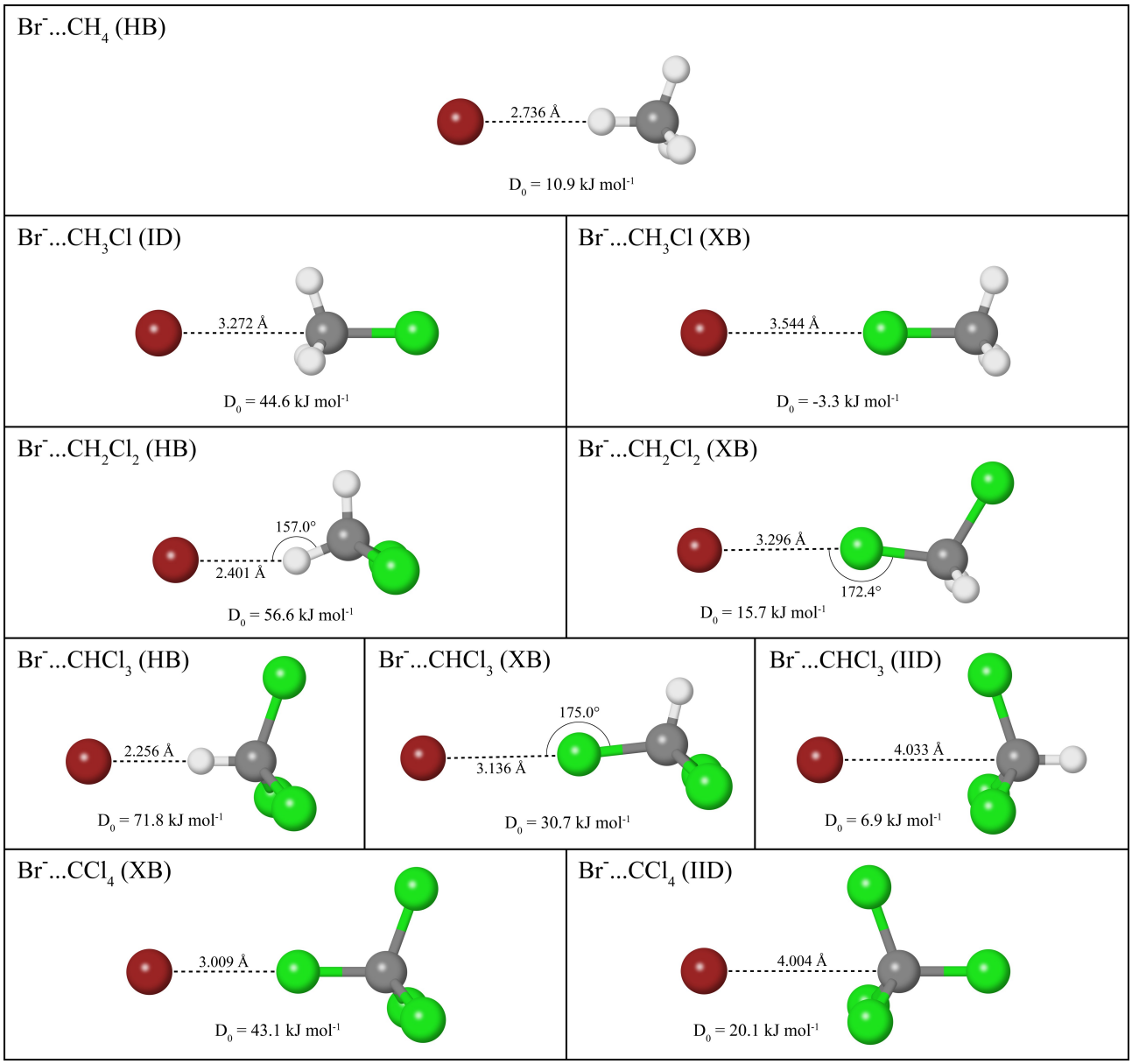

Figure 2. Anion complexes optimised at CCSD(T)/AVTZ level of theory. Associated dissociation energies for each structure are included from Table 2.

for the $Br^-\cdots CCl_4$ complex. A general trend observed throughout the anion structures is that the bond length associated with the van der Waals interaction decreases with increasing chlorination of the methane molecule. For complexes interacting via hydrogen bonding, this is seen as a decrease in the Br–H bond length from 2.736 Å for $Br^-\cdots CH_4$, to 2.256 Å for $Br^-\cdots CHCl_3$, whereas for halogen bond interactions there is a decrease in the Br–Cl bond length from 3.544 Å to 3.009 Å.

The binding motifs observed for the anion complexes have also been shown previously in literature. Three structures have been described for the $Br^-\cdots CH_4$ complex, but only the hydrogen bonded complex is a minimum structure,[73] and has been confirmed by experimental IR studies.[74,75] The two structures optimised for the $Br^-\cdots CH_3Cl$ complex have the same binding motifs as S_N2 reaction adducts.[76,77] The hydrogen bond motif observed for the $Br^-\cdots CH_2Cl_2$ and $Br^-\cdots CHCl_3$ complexes has been shown to also exist in triangular hydrogen and halogen bonded complexes involving CBr_4.[78] The halogen bond motif for $Br^-\cdots CHCl_3$ is similar to that seen for the $Br^-\cdots CHBr_3$ complex,[79] while $Br^-\cdots CH_2Cl_2$ (XB) has been studied previously.[80] A study pertaining to the $Cl^-\cdots CCl_4$ complex also found the XB and IID binding motifs as observed in this study.[67]

Table 2 presents energetics associated with each anion complex, calculated in accordance with the W1w protocol from CCSD(T)/AVTZ geometries to estimate the complete basis set energies, and as such are referred to as CCSD(T)/CBS. Included are vertical detachment energies (VDE) and dissociation energies (D_0). The D_0 is defined as the zero-point corrected difference in electronic energy between the complex and its bare

Table 2. Theoretical dissociation energies (D_0), simulated vertical detachment energies (VDE), and predicted stabilisation energies (E_{stab}) of the anion complexes calculated in accordance with the W1w protocol from CCSD(T)/AVTZ geometries, referred to as CCSD(T)/CBS.

Complex	Symmetry	D_0	VDE		E_{stab}
		[kJ mol^{-1}]	$^2P_{3/2}$ [eV]	$^2P_{1/2}$ [eV]	[eV]
$Br^-\cdots CH_4$ (HB)	C_{3v}	10.9	3.46	3.92	0.10
$Br^-\cdots CH_3Cl$ (ID)	C_{3v}	44.6	3.80	4.25	0.43
$Br^-\cdots CH_3Cl$ (XB)	C_{3v}	−3.3	3.28	3.74	−0.08
$Br^-\cdots CH_2Cl_2$ (HB)	C_s	56.6	3.96	4.42	0.60
$Br^-\cdots CH_2Cl_2$ (XB)	C_s	15.7	3.50	3.96	0.14
$Br^-\cdots CHCl_3$ (HB)	C_{3v}	71.8	4.11	4.57	0.75
$Br^-\cdots CHCl_3$ (XB)	C_s	30.7	3.68	4.14	0.32
$Br^-\cdots CHCl_3$ (IID)	C_{3v}	6.9	3.33	3.78	−0.04
$Br^-\cdots CCl_4$ (XB)	C_{3v}	43.1	3.84	4.30	0.48
$Br^-\cdots CCl_4$ (IID)	C_{3v}	20.1	3.51	3.97	0.15

substituents. The VDE is the amount of energy required to detach an electron from the bromide anion in each complex in the Franck–Condon region to either of the perturbed ^2P states of the bromine, *i.e.*, $^2P_{3/2}$ and $^2P_{1/2}$.

As observed in Table 2, generally complexes with higher D_0 values also predict higher VDE values. The best example of this is $Br^-\cdots CHCl_3$ (HB), which is the most tightly bound anion complex in this study with a D_0 of 71.8 kJ mol^{-1}, predicting the largest $^2P_{3/2}$ VDE of 4.11 eV. This can be explained by the three chlorine atoms, which due to the electron withdrawing capacity of chlorine will contribute to a large dipole moment across the molecule, resulting in electron deficiency on the lone hydrogen atom. The bromide interaction with the hydrogen forms a strong hydrogen bond, and thus a D_0 of 71.8 kJ mol^{-1}. Conversely, the least tightly bound complex is $Br^-\cdots CH_3Cl$ (XB) with a D_0 of −3.3 kJ mol^{-1}, the only complex in this study that has a negative dissociation energy. This is largely due to the methyl hydrogens being a poor electron withdrawing group from the lone chlorine atom, thereby forming a relatively unstable halogen bond. However, despite a negative D_0, this complex is a local minimum as opposed to the global minimum $Br^-\cdots CH_3Cl$ (ID). This can be explained by a transition structure that exists as the bromide anion linearly approaches the chlorine atom of CH_3Cl, which has a central barrier of approximately 8.0 kJ mol^{-1}.

Some trends can be drawn from the D_0 values. The first is that when comparing a type of interaction, such as hydrogen bonding, increasing the chlorination of the methane molecule results in an increase in the D_0 value of the complex. This is shown through the hydrogen bond interactions, which increase from 10.9 kJ mol^{-1} for the $Br^-\cdots CH_4$ complex, to 71.8 kJ mol^{-1} for the $Br^-\cdots CHCl_3$ complex. Similarly for halogen bond interactions, the D_0 value increases from −3.3 kJ mol^{-1} for the $Br^-\cdots CH_3Cl$ complex, to 43.1 kJ mol^{-1} for the $Br^-\cdots CCl_4$ complex. However, this increase is non-linear, as the difference between the halogen bonded $Br^-\cdots CH_2Cl_2$ and $Br^-\cdots CH_3Cl$ complexes is 19.0 kJ mol^{-1}, whereas for the halogen bonded $Br^-\cdots CHCl_3$ and $Br^-\cdots CH_2Cl_2$ complexes the difference is only 15.0 kJ mol^{-1}, and likewise this difference decreases to 12.4 kJ mol^{-1} for the halogen bonded $Br^-\cdots CCl_4$ and $Br^-\cdots CHCl_3$ complexes. This trend appears to hold for the hydrogen bonded complexes as well, so it appears that additional chlorine atoms have a diminishing increase in the stability of the complex, regardless of the type of interaction binding the bromide-chloromethane complex. Interestingly, another trend can be drawn from the D_0 values, in that the hydrogen bonded complexes are approximately 41.0 kJ mol^{-1} more tightly bound than the halogen bonded complexes, based on $Br^-\cdots CH_2Cl_2$ and $Br^-\cdots CHCl_3$. Similarly, comparing $Br^-\cdots CHCl_3$ and $Br^-\cdots CCl_4$, the halogen bonded complexes are approximately 23.4 kJ mol^{-1} more tightly bound than the ion-induced dipole complexes.

Neutral Complexes

While the anion complexes are formed in the experimental apparatus of this study, detachment of an electron from the bromide anion will form a neutral bromine-molecule complex. The neutral complexes were therefore studied to determine whether the binding motifs change relative to the anion complexes. Presented in Figure 3 are the corresponding neutral complex structures optimised at the MP2/AVQZ level of theory, with W1w extrapolated dissociation energies summarised in Table 3. A lower level of theory is used in the geometry optimisations relative to the anion complexes, as the neutral complexes are open-shell systems and require significantly more computational effort than the anion complexes. This is especially true for those containing larger numbers of basis functions ($CHCl_3$ or CCl_4). However, a dataset of W1w extrapolated energies determined from MP2/AVQZ geometries for the anion complexes is included in the supporting information, which have little deviation from the dataset determined from CCSD(T)/AVTZ geometries in the main text. While an unrestricted wavefunction reference is used in these calculations involving the neutral complexes, the amount of spin contamination present in these open-shell systems appears to be low, with the highest $\langle \widehat{S}^2 \rangle$ value reported as 0.7604. A full list of

Research Article
doi.org/10.1002/cphc.202200733

Chemistry Europe
European Chemical Societies Publishing

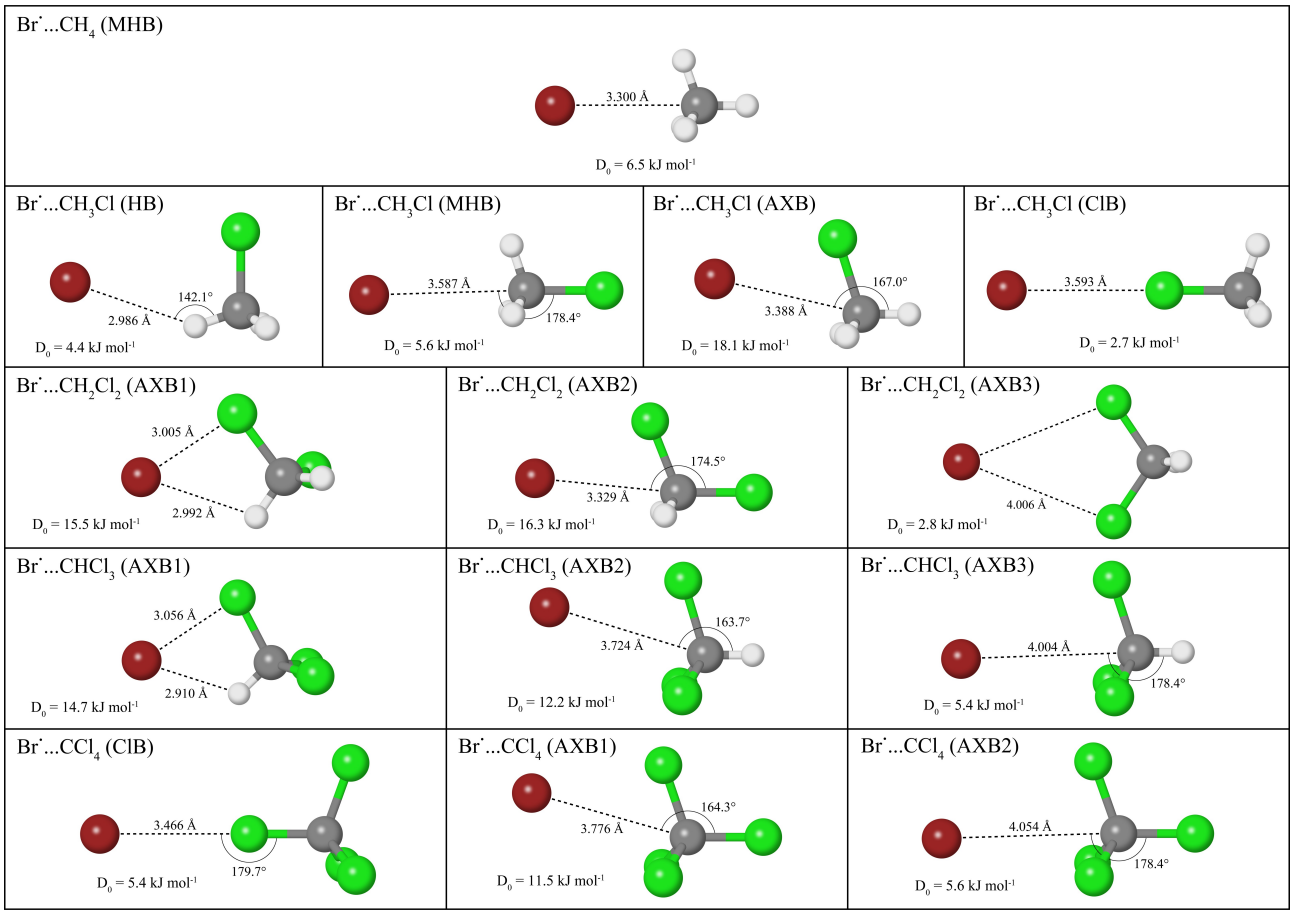

Figure 3. Neutral complexes optimised at MP2/AVQZ level of theory. Associated dissociation energies for each structure are included from Table 3.

Table 3. Theoretical dissociation energies (D_0) of the neutral complexes calculated in accordance with the W1w protocol from MP2/AVQZ geometries, referred to as CCSD(T)/CBS.

Complex	Symmetry	D_0 [kJ mol^{-1}]
Br•···CH_4 (MHB)	C_{3v}	6.5
Br•···CH_3Cl (HB)	C_s	4.4
Br•···CH_3Cl (MHB)	C_s	5.6
Br•···CH_3Cl (AXB)	C_s	18.1
Br•···CH_3Cl (ClB)	C_s	2.7
Br•···CH_2Cl_2 (AXB1)	C_1	15.5
Br•···CH_2Cl_2 (AXB2)	C_s	16.3
Br•···CH_2Cl_2 (AXB3)	C_{2v}	2.8
Br•···$CHCl_3$ (AXB1)	C_1	14.7
Br•···$CHCl_3$ (AXB2)	C_s	12.2
Br•···$CHCl_3$ (AXB3)	C_s	5.4
Br•···CCl_4 (ClB)	C_s	5.4
Br•···CCl_4 (AXB1)	C_s	11.5
Br•···CCl_4 (AXB2)	C_s	5.6

predicted $\langle \widehat{S^2} \rangle$ values are reported in the supporting information. Additionally, the neutral potential energy surface is typically much flatter with respect to the anion surface due to the absence of charge interactions. In this region, small energy gradients result in negligible effects on the e_{BE} of complexes undergoing comparatively large atomic displacements. For these reasons, the MP2/AVQZ geometries were deemed sufficient for determining the structural binding motifs and overall stability of the neutral complexes, providing a benchmark for future studies.

When bromine interacts with a chloromethane, several binding motifs were located. The most common is when bromine interacts with the electron-rich equatorial belt of the chlorine atom, denoted an analogous halogen bond (AXB). This interaction is observed in nine different minima: one Br•···CH_3Cl complex, all three Br•···CH_2Cl_2 complexes, all three Br•···$CHCl_3$ complexes, and two of the Br•···CCl_4 complexes. Bromine interacts linearly with a chlorine atom in two neutral complexes, denoted as chlorine bound or ClB, those being Br•···CH_3Cl (ClB) and Br•···CCl_4 (ClB), while bromine interacts with one of the methyl hydrogens in the Br•···CH_3Cl (HB) complex. Bromine can also interact with the three methyl hydrogen atoms, as shown for one of the Br•···CH_3Cl complexes (denoted as methyl hydrogen bound or MHB), an interaction almost identical to the lone structure identified for the Br•···CH_4 complex.

Several of the neutral structures have binding motifs similar to those studied previously. The Br + CH_4 potential energy

surface has been studied extensively, where the $Br^{\bullet}\cdots CH_4$ (MHB) complex was shown to be the global minimum.[81] The four $Br^{\bullet}\cdots CH_3Cl$ complexes found in this study have similar binding motifs to those found in a study pertaining to CH_3Cl dimer complexes, where instead of the CH_3Cl moiety interacting with atomic bromine, the interaction occurs with the chlorine atom of the other CH_3Cl molecule.[82] The lone $Br^{\bullet}\cdots CCl_3Br$ neutral structure shown in a study by Bowen and co-workers features atomic bromine interacting with the bromine atom of CCl_3Br,[68] an interaction similar to what is shown in this study for the $Br^{\bullet}\cdots CCl_4$ (AXB1) complex.

Of the structures found for the neutral complexes, the complexes interacting via analogous halogen bonding typically have the highest D_0 values, and therefore are predicted to be the most stable. However, three of the nine analogous halogen bond complexes have D_0 values lower than 6 kJ mol^{-1}, those being $Br^{\bullet}\cdots CH_2Cl_2$ (AXB3), $Br^{\bullet}\cdots CHCl_3$ (AXB3), and $Br^{\bullet}\cdots CCl_4$ (AXB2). One possible explanation for this is that the interaction occurs with multiple chlorine atoms, so the complexes are less tightly bound. As for the remaining structures, they are all less tightly bound due to the electrophilic bromine interacting with regions of the molecule that are relatively electron-deficient, such as interactions with hydrogen atoms or at the side of the chlorine atom opposite the C–Cl covalent bond.

Contrary to the anion complexes, the general trend observed among the neutral complexes is that for any given interaction the complex becomes less tightly bound with increasing chlorination of the base methane molecule, an example of which is $Br^{\bullet}\cdots CH_3Cl$ (MHB) which has a lower D_0 than $Br^{\bullet}\cdots CH_4$ (MHB). This is because more chlorine atoms will result in less electron density concentrated in one region of the molecule, therefore making interactions with electrophilic bromine less favourable. This also explains why $Br^{\bullet}\cdots CH_3Cl$ (AXB) is the most stable neutral complex, as electron density will mostly be concentrated on the lone chlorine atom, hence the relatively large D_0 of 18.1 kJ mol^{-1}. Interestingly, the only exception to this trend is that $Br^{\bullet}\cdots CCl_4$ (ClB) is more stable than $Br^{\bullet}\cdots CH_3Cl$ (ClB). Based on theoretical dissociation energies, hydrogen bonding is a more stable interaction than halogen bonding when a nucleophile is interacting with a solvent molecule, such as in the case of the bromide anion complexes. However, in the case of an electrophile such as atomic bromine the opposite seems to occur, where the analogous halogen bond is a more stable interaction than the interactions involving solely the hydrogen atoms.

Rationalisation of Experimental Data

A formal assignment of theoretical structures to the experimental photoelectron spectra is given in Table 4, where the experimental photoelectron peak locations are compared to the theoretical vertical detachment energies computed from the optimised anion geometries (as shown in Figure 2). Zheng and co-workers found that the $^2P_{3/2}$ and $^2P_{1/2}$ peaks of the $Br^-\cdots CH_4$ complex lie at 3.45 eV and 3.91 eV respectively.[70] This study has predicted that the $Br^-\cdots CH_4$ complex has only one possible structure, a hydrogen bond motif, with theoretical VDE values of 3.46 eV and 3.92 eV which are in good agreement with experiment.[70] The two minima found for the $Br^-\cdots CH_3Cl$ complex include the ion-dipole bound structure, with predicted peaks at 3.80 eV and 4.25 eV, and the halogen bond structure which is predicted to lie at 3.28 eV and 3.74 eV. Experimentally, the peak locations of the $Br^-\cdots CH_3Cl$ complex are found at 3.78 eV and 4.24 eV, and upon comparison with the *ab initio* calculations, the ion-dipole bound structure is in close agreement with experiment, with no evidence of any peaks that would indicate the presence of the halogen bond structure. Regarding the $Br^-\cdots CH_2Cl_2$ complex, the predicted VDE values of the hydrogen bond structure at 3.96 eV and 4.42 eV lie in close agreement with the observed experimental peak locations at 3.95 eV and 4.40 eV, while the lack of a photodetachment peak at 3.50 eV is evidence that the halogen bond structure is not present experimentally. Of the three possible minima structures corresponding to the $Br^-\cdots CHCl_3$ complex, the theoretical VDE values calculated for the hydrogen bond structure at 4.11 eV

Table 4. Comparison of experimental and theoretical peak locations. The experimental values are from Table 1, whereas the theoretical values are from Table 2 and are calculated in accordance with the W1w protocol from CCSD(T)/AVTZ geometries, referred to as CCSD(T)/CBS.

	Experimental		Binding Motif	Theoretical	
	$^2P_{3/2}$ [eV]	$^2P_{1/2}$ [eV]		$^2P_{3/2}$ [eV]	$^2P_{1/2}$ [eV]
$Br^-\cdots CH_4$	3.45[a]	3.91[a]	HB	3.46	3.92
$Br^-\cdots CH_3Cl$	3.78	4.24	ID XB	3.80 3.28	4.25 3.74
$Br^-\cdots CH_2Cl_2$	3.95	4.40	HB XB	3.96 3.50	4.42 3.96
$Br^-\cdots CHCl_3$	4.09	4.51	HB XB IID	4.11 3.68 3.33	4.57 4.14 3.78
$Br^-\cdots CCl_4$	3.84	4.30	XB IID	3.84 3.51	4.30 3.97

[a] Zheng and co-workers.[70]

and 4.57 eV have the closest agreement to the experimental peak locations found at 4.09 eV and 4.51 eV. The VDE values calculated for the halogen bond structure, 3.68 eV and 4.14 eV, and for the ion-induced dipole structure, 3.33 eV and 3.78 eV, do not agree with the experimental data. As for the $Br^-\cdots CCl_4$ complex, the halogen bond structure predicts VDE values at 3.84 eV and 4.30 eV, which are in excellent agreement with the experimental peak locations that are also found at 3.84 eV and 4.30 eV, whereas the theoretical peak locations of 3.51 eV and 3.97 eV calculated for the ion-induced dipole complex do not agree with the experimental data.

Further evidence to support the assignment of each structure to the experimental photoelectron spectra can be found through the experimental E_{stab} values and the theoretical D_0 values. This is done through a process of elimination, where structures that are predicted to be less tightly bound theoretically than structures already assigned to previous experiments in the chloromethanes series are considered unlikely to be the structure observed experimentally. Take $Br^-\cdots CH_4$, which experimentally has a small E_{stab} of 0.09 eV.[70] For the lone hydrogen bound structure, this small shift is also reflected in the D_0 value, calculated to be 10.9 kJ mol^{-1} at CCSD(T)/CBS level of theory. As there are no other minima structures to consider, $Br^-\cdots CH_4$ (HB) is the only structure that can be assigned to the spectrum. When considering the $Br^-\cdots CH_3Cl$ spectrum, the experimental E_{stab} value of 0.42 eV is much higher than that observed in the $Br^-\cdots CH_4$ spectrum, and of the two structures predicted theoretically only the ion-dipole $Br^-\cdots CH_3Cl$ complex has a higher D_0 than the hydrogen bound $Br^-\cdots CH_4$ complex. The other structure, $Br^-\cdots CH_3Cl$ (XB), is predicted to be less stable in terms of D_0 relative to $Br^-\cdots CH_4$ (HB), and if this was true then the peaks observed in the $Br^-\cdots CH_3Cl$ spectrum would have to lie at lower e_{BE} than what is actually observed, thus the halogen bond structure is inappropriate to assign to the $Br^-\cdots CH_3Cl$ spectrum. Applying this logic to the remaining spectra, it can be shown that $Br^-\cdots CH_2Cl_2$ (HB), $Br^-\cdots CHCl_3$ (HB), and $Br^-\cdots CCl_4$ (XB) are the most appropriate structures to assign to their respective spectra, the same structures that are predicted to have VDEs that agree with the experimental peaks. Therefore, based on the assignment of optimised structures to the experimental spectra in this study, there is strong evidence to suggest that hydrogen bonding interactions are favoured over halogen bonding interactions in anion-molecule complexes when both hydrogen atoms and chlorine atoms are present in the solvent molecule.

For some of the assigned structures, there is a small deviation between the photodetachment peak locations observed experimentally, and the predicted VDE values, such as in the case of $Br^-\cdots CHCl_3$. The main reason for this is likely due to a small change in the spin-orbit splitting of bromine when forming a complex. It is known that the spin-orbit constant of bare bromide is approximately 0.46 eV,[83] and when calculating the theoretical VDE for a bromide complex it is assumed here that this value does not change, hence why it is not factored into the calculation. While there appears to be negligible change in spin-orbit splitting for $Br^-\cdots CH_3Cl$ and $Br^-\cdots CCl_4$ given the poor resolution of our experimental apparatus, a spin-orbit splitting of approximately 0.45 eV is observed for the $Br^-\cdots CH_2Cl_2$ complex, and an even smaller spin-orbit splitting of 0.42 eV is observed for the $Br^-\cdots CHCl_3$ complex. Interestingly, Zheng and co-workers observed an increased spin-orbit splitting of approximately 0.01 eV for the $Br^-\cdots CH_4$ complex relative to bare bromide.[70] A computational method that could be used to calculate theoretical energies of the spin states for each complex to compare to experimental values is the CASSCF method, however this is beyond the scope of this study.

Previous photoelectron spectroscopy studies regarding similar halide-chloromethane complexes can be compared directly to the results found in this study. The $Cl^-\cdots CCl_4$ complex was found to have a VDE at 4.22 eV, corresponding to an E_{stab} of approximately 0.58 eV with respect to the bare chloride spectrum.[67] Bowen and co-workers studied the $Br^-\cdots CCl_3Br$ complex, and found that the $^2P_{3/2}$ peak shifted from 3.37 eV for Br^-, to 4.21 eV for the complex, an E_{stab} of approximately 0.84 eV.[68] Mabbs and co-workers investigated the $I^-\cdots CH_3Cl$ complex, and found the $^2P_{3/2}$ peak to lie at 3.41 eV, corresponding to an E_{stab} of approximately 0.35 eV.[84] Similarly, the $I^-\cdots CH_2Cl_2$ complex has been studied, where the $^2P_{3/2}$ peak was found at 3.52 eV, which is an E_{stab} of approximately 0.46 eV.[85] The main comparisons that can be made from these various studies is that the halide impacts the strength of the intermolecular interaction, which typically follows a trend of $Cl^- > Br^- > I^-$.[50,86,87] This trend is highlighted between the $X^-\cdots CCl_4$ complexes, where the E_{stab} value found for $Br^-\cdots CCl_4$ of 0.48 eV is lower than the 0.58 eV found for $Cl^-\cdots CCl_4$. Similarly, the E_{stab} values for $Br^-\cdots CH_3Cl$ and $Br^-\cdots CH_2Cl_2$ of 0.42 eV and 0.59 eV respectively, are higher than those found for $I^-\cdots CH_3Cl$ and $I^-\cdots CH_2Cl_2$ of 0.35 eV and 0.46 eV respectively. As for the $Br^-\cdots CCl_3Br$ complex, the E_{stab} of 0.84 eV is much higher than that found for the $Br^-\cdots CCl_4$ complex in this study. This is due to the bromide forming a halogen bond with a different atom, which in the case of $Br^-\cdots CCl_3Br$ is a bromide-bromine halogen bond. The reason this is a stronger interaction is due to the weaker electron withdrawing capacity of bromine relative to chlorine, so the three chlorine atoms in CCl_3Br withdraw electron density from the bromine atom more readily, resulting in a region of lower electron density at the side of the bromine atom opposite the C–Br covalent bond, allowing for a more favourable interaction with a nucleophile relative to a chlorine atom in CCl_4.

Conclusions

This study has investigated gas-phase complexes pertaining to the bromide anion interacting with the four chloromethane molecules, CH_3Cl, CH_2Cl_2, $CHCl_3$, and CCl_4. Experimental photoelectron spectra were recorded for each bromide chloromethane complex, of which the E_{stab} values were determined to be 0.42 eV for $Br^-\cdots CH_3Cl$, 0.59 eV for $Br^-\cdots CH_2Cl_2$, 0.73 eV for $Br^-\cdots CHCl_3$, and 0.48 eV for $Br^-\cdots CCl_4$. This large solvent shift found for each complex indicates that the bromide anion is bound by strong non-covalent interactions.

The types of non-covalent interactions were investigated using *ab initio* calculations to determine the most stable binding motifs for each complex, which includes hydrogen bonding and halogen bonding. The theoretical VDEs for each complex were compared to the photoelectron spectra, which found that an ion-dipole motif was the most stable $Br^-\cdots CH_3Cl$ complex, whereas a hydrogen bond motif was determined to be the most stable interaction for the $Br^-\cdots CH_2Cl_2$ and $Br^-\cdots CHCl_3$ complex. For the $Br^-\cdots CCl_4$ complex, the most stable interaction was found to be the halogen bond.

Additionally, computational work was conducted on the neutral bromine chloromethane complexes to determine whether the types of favourable interactions would differ relative to their anion counterparts. The analogous halogen bond was found to be the most stable interaction for all bromine chloromethane complexes, indicated by the larger dissociation energies relative to the other structures. Thus, there is experimental evidence that hydrogen bond interactions are predominantly favoured over halogen bond interactions for the anion complexes, where a nucleophile is interacting with the chloromethane, whereas the analogous halogen bond interactions appear to be more stable than interactions solely with hydrogen atoms for the neutral complexes, where instead an electrophile is interacting with the chloromethane.

Experimental Section

The experimental apparatus comprises of a Wiley-McLaren style time-of-flight mass spectrometer,[88] coupled to a photoelectron spectrometer that has a Cheshnovsky *et al.* magnetic bottle-neck design.[72] Previous publications have outlined the overall experimental setup in detail,[89–91] so only specific information regarding the current work will be provided.

Gas mixtures required to form the various bromide-chloromethane complexes contain a total pressure of 400 kPa which consists of mostly argon, with trace amounts of dibromomethane as the bromide donor introduced into the gas mixture by way of vapour pressure. The vapour pressure associated with dichloromethane, trichloromethane, and tetrachloromethane was used to introduce three of the four solvent species into their respective gas mixtures, whereas approximately 7 kPa of monochloromethane was introduced into its respective gas mixture. A piezoelectric nozzle pulses the gas mixture into the spectrometer, where the resultant supersonic expansion is intersected by a beam of electrons originating from a hot rhenium filament, allowing the gas species to undergo dissociative electron attachment processes that form the desired anion species, including van der Waals complexes. All anion species are accelerated down a time-of-flight tube to achieve mass separation, where the desired bromide-chloromethane complex is selected for photoelectron spectroscopy experiments. The bromide-chloromethane complexes are intersected with 266 nm (4.66 eV) laser radiation, produced from the fourth harmonic of a Nd:YAG Spectra Physics Quanta Ray Pro, and the detached photoelectrons are guided to a detector. The time-of-flight associated with the arrival of the photoelectrons are converted to electron kinetic energy, which is used to calculate the electron binding energy based on the known photon energy of the laser radiation.

Spectral intensities need to be readjusted to account for the non-linear conversion from time-of-flight to kinetic energy, which involves multiplying the spectral intensities by their time-of-flight cubed (t^3). The photoelectron spectra associated with each bromide-chloromethane complex are the result of multiple background-subtracted spectra summed together, where each individual spectrum consists of 10,000 laser shots. Based on the known $^2P_{3/2}$ and $^2P_{1/2}$ spin-orbit states of atomic bromine,[83,92] calibration spectra associated with the bare bromide anion are recorded to account for any drift in electron kinetic energy.

Computational Methods

In all calculations, Dunning's augmented, correlation consistent basis sets (aug-cc-pVXZ where X = D, T, Q) were applied to carbon and hydrogen atoms,[93] with chlorine atoms being allocated its respective aug-cc-pV(X + d)Z basis sets,[94,95] and the equivalent pseudo-potential aug-cc-pVXZ-PP basis sets being applied to bromine atoms.[96,97] Collectively, these basis sets are referred to as AVXZ in both the main text and the supporting information. The Gaussian 09 program[98] was used for calculations involving the MP2/AVQZ geometries dataset for both the anion and neutral complexes. The CFOUR computational chemistry program[99] was used for calculations involving the CCSD(T)/AVTZ geometries dataset for the anion complexes. Vibrational frequency analysis calculations at the equivalent level of theory were performed for each optimised geometry to determine whether the structure was a minimum on the potential energy surface. CCSD(T) single point energy calculations were performed for every structure in both MP2/AVQZ and CCSD(T)/AVTZ datasets, using AVDZ, AVTZ and AVQZ basis sets in order to perform a two-point basis set extrapolation in accordance with the Weizmann (W1w) protocol.[100,101] The W1w protocol allows for an approximation of the CCSD(T)/CBS energies, and thus any energies reported that are extrapolated using this method are referred to as CCSD(T)/CBS.

All calculations involving neutral open-shell complexes, including the theoretical vertical detachment energy (VDE) calculations, make use of unrestricted Hartree-Fock theory. The theoretical VDE values were determined from single point energy calculations of an optimised anion structure, where the charge and multiplicity are altered to simulate the detachment of an electron. Electron affinities (EA), while not reported in the main article but are present in the supporting information, were determined from single point energy calculations, being the difference in energy between an optimised neutral structure and the most stable optimised anion structure for a given chloromethane complex (e.g. $Br^-\cdots CHCl_3$ (HB) is the most stable anion structure when determining EA of $Br^\bullet\cdots CHCl_3$ neutral structures). Both VDE and EA values are split into $^2P_{3/2}$ and $^2P_{1/2}$ spin-orbit states based on the experimental spin-orbit constant of bromine.[83] A shift factor of −0.013 eV is also applied to the VDE and EA values, determined from the difference in energy between the experimental and theoretical $^2P_{3/2}$ electronic state of atomic bromine.[92]

Acknowledgements

This research was undertaken with the assistance of computational resources from the Pople high-performance computing cluster of the Faculty of Science at the University of Western Australia. The Australian Research Council is acknowledged for funding the laser installation under the LIEF scheme (LE110100093). The School of Molecular Sciences and the Faculty of Science are acknowledged for financial support. H.T.R. thanks the support of a Research Training Program (RTP) scholarship funded by the Australian Government, C.T.H. acknowledges the

UWA Dean's Excellence in Science PhD Scholarship, T.R.C. thanks the support of a Research Training Program (RTP) scholarship funded by the Australian Government, and P.D.W. acknowledges the support of the Center for Materials Crystallography at Aarhus University in Denmark, funded by the Danish National Research Foundation (DNRF93). Open Access publishing facilitated by The University of Western Australia, as part of the Wiley - The University of Western Australia agreement via the Council of Australian University Librarians.

Conflict of Interest

The authors declare no conflict of interest.

Data Availability Statement

The data that support the findings of this study are available in the supplementary material of this article.

Keywords: *ab initio* calculations · halides · hydrogen bonds · noncovalent interactions · photoelectron spectroscopy

[1] D. Braga, F. Grepioni, *Acc. Chem. Res.* **2000**, *33*, 601–608.
[2] G. R. Desiraju, *Acc. Chem. Res.* **2002**, *35*, 565–573.
[3] P. Dydio, J. N. H. Reek, *Chem. Sci.* **2014**, *5*, 2135–2145.
[4] C. A. Schoenbaum, D. K. Schwartz, J. Will Medlin, *Acc. Chem. Res.* **2014**, *47*, 1438–1445.
[5] K. T. Mahmudov, A. J. L. Pombeiro, *Chem. Eur. J.* **2016**, *22*, 16356–16398.
[6] E. Persch, O. Dumele, F. Diederich, *Angew. Chem. Int. Ed.* **2015**, *54*, 3290–3327; *Angew. Chem.* **2015**, *127*, 3341–3382.
[7] M. Eisenstein, Z. Shakked, *J. Mol. Biol.* **1995**, *248*, 662–678.
[8] K. E. Routledge, G. G. Tartaglia, G. W. Platt, M. Vendruscolo, S. E. Radford, *J. Mol. Biol.* **2009**, *389*, 776–786.
[9] P. Muller, *Pure Appl. Chem.* **1994**, *66*, 1077–1184.
[10] Y. Mao, P. R. Horn, M. Head-Gordon, *Phys. Chem. Chem. Phys.* **2017**, *19*, 5944–5958.
[11] K. E. Riley, P. Hobza, *Phys. Chem. Chem. Phys.* **2013**, *15*, 17742–17751.
[12] U. Adhikari, S. Scheiner, *J. Phys. Chem. A* **2014**, *118*, 3183–3192.
[13] S. Scheiner, *J. Chem. Phys.* **2011**, *134*, 094315.
[14] H. Hernández-Soto, F. Weinhold, J. S. Francisco, *J. Chem. Phys.* **2007**, *127*, 164102.
[15] L. E. Prevette, T. E. Kodger, T. M. Reineke, M. L. Lynch, *Langmuir* **2007**, *23*, 9773–9784.
[16] Y. Liu, W. Zhao, C.-H. Chen, A. H. Flood, *Science* **2019**, *365*, 159–161.
[17] E. Arunan, G. R. Desiraju, R. A. Klein, J. Sadlej, S. Scheiner, I. Alkorta, D. C. Clary, R. H. Crabtree, J. J. Dannenberg, P. Hobza, H. G. Kjaergaard, A. C. Legon, B. Mennucci, D. J. Nesbitt, *Pure Appl. Chem.* **2011**, *83*, 1637–1641.
[18] B. E. Rocher-Casterline, L. C. Chán g, A. K. Mollner, H. J. Reisler, *Chem. Phys.* **2011**, *134*, 211101.
[19] P. Gilli, L. Pretto, V. Bertolasi, G. Gilli Acc, *Chem. Res.* **2009**, *42*, 33–44.
[20] Y. Lu, T. Shi, Y. Wang, H. Yang, X. Yan, X. Luo, H. Jiang, W. Zhu, *J. Med. Chem.* **2009**, *52*, 2854–2862.
[21] R. L. Sutar, S. M. Huber, *ACS Catal.* **2019**, *9*, 9622–9639.
[22] R. Wilcken, M. O. Zimmermann, A. Lange, A. C. Joerger, F. M. Boeckler, *J. Med. Chem.* **2013**, *56*, 1363–1388.
[23] S. J. Stropoli, T. Khuu, J. P. Messinger, N. V. Karimova, M. A. Boyer, I. Zakai, S. Mitra, A. L. Lachowicz, N. Yang, S. C. Edington, R. B. Gerber, A. B. McCoy, M. A. Johnson, *J. Phys. Chem. Lett.* **2022**, *13*, 2750–2756.
[24] P. Politzer, P. Lane, M. C. Concha, Y. Ma, J. S. Murray, *J. Mol. Model.* **2007**, *13*, 305–311.
[25] G. R. Desiraju, P. S. Ho, L. Kloo, A. C. Legon, R. Marquardt, P. Metrangolo, P. Politzer, G. Resnati, K. Rissanen, *Pure Appl. Chem.* **2013**, *85*, 1711–1713.
[26] T. Clark, M. Hennemann, J. S. Murray, P. Politzer, *J. Mol. Model.* **2007**, *13*, 291–296.
[27] P. Politzer, J. S. Murray, *ChemPhysChem* **2013**, *14*, 278–294.
[28] C. Wang, L. Guan, D. Danovich, S. Shaik, Y. Mo, *J. Comput. Chem.* **2016**, *37*, 34–45.
[29] S. Tsuzuki, A. Wakisaka, T. Ono, T. Sonoda, *Chem. Eur. J.* **2011**, *18*, 951–960.
[30] M. A. Perkins, G. S. Tschumper, *J. Phys. Chem. A* **2022**, *126*, 3688–3695.
[31] D. J. Pascoe, K. B. Ling, S. L. Cockroft, *J. Am. Chem. Soc.* **2017**, *139*, 15160–15167.
[32] U. Adhikari, S. Scheiner, *Chem. Phys. Lett.* **2011**, *514*, 36–39.
[33] C. T. Haakansson, T. R. Corkish, P. D. Watson, H. T. Robinson, T. Tsui, A. J. McKinley, D. A. Wild, *ChemPhysChem* **2021**, *22*, 808–812.
[34] A. Bauza, T. J. Mooibroek, A. Frontera, *ChemPhysChem* **2016**, *17*, 1608–1614.
[35] S. Chandra, N. Mahapatra, N. Ramanathan, K. Sundararajan, *J. Phys. Chem. A* **2022**, *126*, 3511–3520.
[36] R. Wysokinski, W. Zierkiewicz, M. Michalczyk, S. Scheiner, *ChemPhysChem* **2022**, *23*, e202200173.
[37] A. Bauza, D. Quinonero, P. M. Deyá, A. Frontera, *CrystEngComm* **2013**, *15*, 3137–3144.
[38] S. Scheiner, *Int. J. Quantum Chem.* **2012**, *113*, 1609–1620.
[39] M. Hou, Q. Li, S. Scheiner, *ChemPhysChem* **2019**, *20*, 1978–1984.
[40] E. Corradi, S. V. Meille, M. T. Messina, P. Metrangolo, G. Resnati, *Angew. Chem. Int. Ed.* **2000**, *39*, 1782–1786; *Angew. Chem.* **2000**, *112*, 1852–1856.
[41] C. C. Robertson, J. S. Wright, E. J. Carrington, R. N. Perutz, C. A. Hunter, L. Brammer, *Chem. Sci.* **2017**, *8*, 5392–5398.
[42] Q. Li, Q. Lin, W. Li, J. Cheng, B. Gong, J. Sun, *ChemPhysChem* **2008**, *9*, 2265–2269.
[43] C. M. Trudinger, D. M. Etheridge, G. A. Sturrock, P. J. Fraser, P. B. Krummel, A. J. McCulloch, *J. Geophys. Res. [Atmos.]* **2004**, *109*, D22310.
[44] P. J. Fraser, B. L. Dunse, A. J. Manning, S. Walsh, R. H. J. Wang, P. B. Krummel, L. P. Steele, L. W. Porter, C. Allison, S. O'Doherty, P. G. Simmonds, J. Mühle, R. F. Weiss, R. G. Prinn, *Environ. Chem.* **2014**, *11*, 77–88.
[45] M. R. Bassford, P. G. Simmonds, G. Nickless, *Anal. Chem.* **1998**, *70*, 958–965.
[46] D. Sherry, A. McCulloch, Q. Liang, S. Reimann, P. A. Newman, *Environ. Res. Lett.* **2018**, *13*, 024004.
[47] W.-T. Tsai, *Toxics* **2017**, *5*, 23.
[48] N. R. Carlon, D. K. Papanastasiou, E. L. Fleming, C. H. Jackman, P. A. Newman, J. B. Burkholder, *Atmos. Chem. Phys.* **2010**, *10*, 6137–6149.
[49] R. Hossaini, M. P. Chipperfield, B. M. Monge-Sanz, N. A. D. Richards, E. Atlas, D. R. Blake, *Atmos. Chem. Phys.* **2010**, *10*, 719–735.
[50] T. R. Corkish, C. T. Haakansson, P. D. Watson, H. T. Robinson, A. J. McKinley, D. A. Wild, *ChemPhysChem* **2021**, *22*, 1316–1320.
[51] C. T. Haakansson, T. R. Corkish, P. D. Watson, D. B. Hart, A. J. McKinley, D. A. Wild, *Chem. Phys. Lett.* **2022**, *793*, 139433.
[52] T. R. Corkish, D. B. Hart, P. D. Watson, A. J. McKinley, D. A. Wild, *J. Mol. Spectrosc.* **2019**, *364*, 111178.
[53] E. V. Bartashevich, Y. V. Matveychuk, E. A. Troitskaya, V. G. Tsirelson, *Comput. Theor. Chem.* **2014**, *1037*, 53–62.
[54] J. Chen, Y. Zheng, A. Melli, L. Spada, T. Lu, G. Feng, Q. Gou, V. Barone, C. Puzzarini, *Phys. Chem. Chem. Phys.* **2020**, *22*, 5024–5032.
[55] B. Nepal, S. Scheiner, *Phys. Chem. Chem. Phys.* **2016**, *18*, 18015–18023.
[56] J. Rézéc, P. Hobza, *Chem. Rev.* **2016**, *116*, 5038–5071.
[57] J. Rézác, *J. Chem. Theory Comput.* **2020**, *16*, 2355–2368.
[58] S. Parthiban, G. de Oliveira, J. M. L. Martin, *J. Phys. Chem. A* **2001**, *105*, 895–904.
[59] E. Alikhani, F. Fuster, B. Madebene, S. J. Grabowski, *Phys. Chem. Chem. Phys.* **2014**, *16*, 2430–2442.
[60] U. Adhikari, S. Scheiner, *J. Phys. Chem. A* **2014**, *118*, 3183–3192.
[61] L. de Azevedo Santos, T. C. Ramalho, T. A. Hamlin, F. M. Bickelhaupt, *J. Comput. Chem.* **2021**, *42*, 688–698.
[62] S. Scheiner, R. Wysokinski, M. Michalczyk, W. Zierkiewicz, *J. Phys. Chem. A* **2020**, *124*, 4998–5006.
[63] S. Scheiner, M. Michalczyk, W. Zierkiewicz, *Chem. Phys.* **2019**, *524*, 55–62.
[64] F. Mbaiwa, M. V. Duzor, J. Wei, R. Mabbs, *J. Phys. Chem. A* **2010**, *114*, 1539–1547.

[65] S. B. King, M. A. Yandell, D. M. Neumark, *Faraday Discuss.* **2013**, *163*, 59–72.
[66] C. T. Haakansson, T. R. Corkish, P. D. Watson, A. J. McKinley, D. A. Wild, *Chem. Phys. Lett.* **2020**, *761*, 138060.
[67] T. R. Corkish, C. T. Haakansson, A. J. McKinley, D. A. Wild, *J. Phys. Chem. Lett.* **2019**, *10*, 5338–5342.
[68] X. Zhang, G. Liu, S. Ciborowski, W. Wang, C. Gong, Y. Yao, K. Bowen, *Angew. Chem. Int. Ed.* **2019**, *58*, 11400–11403; *Angew. Chem.* **2019**, *131*, 11522–11525.
[69] G. Mensa-Bonsu, D. J. Tozer, J. R. R. Verlet, *Phys. Chem. Chem. Phys.* **2019**, *21*, 13977–13985.
[70] M. Cheng, Y. Feng, Y. Du, Q. Zhu, W. Zheng, G. Czako, J. M. Bowman, *J. Chem. Phys.* **2011**, *134*, 191102.
[71] D. W. Arnold, S. E. Bradforth, E. H. Kim, D. M. Neumark, *J. Chem. Phys.* **1995**, *102*, 3510–3518.
[72] O. Cheshnovsky, S. H. Yang, C. L. Pettiette, M. J. Craycraft, R. E. Smalley, *Rev. Sci. Instrum.* **1987**, *58*, 2131–2137.
[73] J. J. Novoa, M.-H. Whangbo, J. M. Williams, *Chem. Phys. Lett.* **1991**, *180*, 241–248.
[74] D. A. Wild, Z. M. Loh, E. J. Bieske, *Int. J. Mass Spectrom.* **2002**, *220*, 273–280.
[75] Z. M. Loh, R. L. Wilson, D. A. Wild, E. J. Bieske, M. S. Gordon, *J. Phys. Chem. A* **2005**, *109*, 8481–8486.
[76] A. Dékány, G. Z. Kovács, G. Czako, *J. Phys. Chem. A* **2021**, *125*, 9645–9657.
[77] H. T. Robinson, T. R. Corkish, C. T. Haakansson, P. D. Watson, A. J. McKinley, D. A. Wild, *ChemPhysChem* **2022**, *23*, e202200278.
[78] Y. Wu, X. Zhao, H. Gao, W. Jin, *Chin. J. Chem. Phys.* **2014**, *27*, 265–273.
[79] S. V. Rosokha, C. L. Stern, J. T. Ritzert, *Chem. Eur. J.* **2013**, *19*, 8774–8788.
[80] D. M. Ivanov, M. A. Kinzhalov, A. S. Novikov, I. V. Ananyev, A. A. Romanova, V. P. Boyarskiy, M. Haukka, V. Y. Kukushkin, *Cryst. Growth Des.* **2017**, *17*, 1353–1362.
[81] G. Czako, *J. Chem. Phys.* **2013**, *138*, 134301.
[82] K. B. Wiberg, *ACS Omega* **2021**, *6*, 15199–15204.
[83] J. L. Tech, *J. Res. Natl. Bur. Stand. Sect. A* **1963**, *67A*, 505–554.
[84] M. V. Duzor, J. Wei, F. Mbaiwa, R. Mabbs, *J. Chem. Phys.* **2010**, *133*, 144303.
[85] J. S. Lasinski, PhD thesis, Washington University in St. Louis (USA), **2013**.
[86] G. Markovich, S. Pollack, R. Giniger, O. Cheshnovsky, *J. Chem. Phys.* **1994**, *101*, 9344–9353.
[87] H. Zhang, W. Cao, Q. Yuan, L. Wang, X. Zhou, S. Liu, X.-B. Wang, *Phys. Chem. Chem. Phys.* **2020**, *22*, 19459–19467.
[88] W. C. Wiley, I. H. McLaren, *Rev. Sci. Instrum.* **1955**, *26*, 1150–1157.
[89] K. M. Lapere, R. J. LaMacchia, L. H. Quak, A. J. McKinley, D. A. Wild, *Chem. Phys. Lett.* **2011**, *504*, 13–19.
[90] D. A. R. Beckham, S. Conran, K. M. Lapere, M. Kettner, A. J. McKinley, D. A. Wild, *Chem. Phys. Lett.* **2015**, *619*, 241–246.
[91] T. R. Corkish, C. T. Haakansson, P. D. Watson, A. J. McKinley, D. A. Wild, *ChemPhysChem* **2021**, *22*, 69–75.
[92] C. Blondel, P. Cacciani, C. Delsart, R. Trainham, *Phys. Rev. A* **1989**, *40*, 3698–3701.
[93] R. A. Kendall, T. H. Dunning Junior, R. J. Harrison, *J. Chem. Phys.* **1992**, *96*, 6796–6806.
[94] D. E. Woon, T. H. Dunning Jr, *J. Chem. Phys.* **1993**, *98*, 1358–1371.
[95] T. H. Dunning Junior, K. A. Peterson, A. K. Wilson, *J. Chem. Phys.* **2001**, *114*, 9244–9253.
[96] K. A. Peterson, D. Figgen, E. Goll, H. Stoll, M. Dolg, *J. Chem. Phys.* **2003**, *119*, 11113–11123.
[97] K. A. Peterson, B. C. Shepler, D. Figgen, H. Stoll, *J. Phys. Chem. A* **2006**, *110*, 13877–13883.
[98] M. J. Frisch, G. W. Trucks, H. B. Schlegel, G. E. Scuseria, M. A. Robb, J. R. Cheeseman, G. Scalmani, V. Barone, B. Mennucci, G. A. Petersson, H. Nakatsuji, M. Caricato, X. Li, H. P. Hratchian, A. F. Izmaylov, J. Bloino, G. Zheng, J. L. Sonnenberg, M. Hada, M. Ehara, K. Toyota, R. Fukuda, J. Hasegawa, M. Ishida, T. Nakajima, Y. Honda, O. Kitao, H. Nakai, T. Vreven, J. A. Montgomery Junior, J. E. Peralta, F. Ogliaro, M. Bearpark, J. J. Heyd, E. Brothers, K. N. Kudin, V. N. Staroverov, R. Kobayashi, J. Normand, K. Raghavachari, A. Rendell, J. C. Burant, S. S. Iyengar, J. Tomasi, M. Cossi, N. Rega, J. M. Millam, M. Klene, J. E. Knox, J. B. Cross, V. Bakken, C. Adamo, J. Jaramillo, R. Gomperts, R. E. Stratmann, O. Yazyev, A. J. Austin, R. Cammi, C. Pomelli, J. W. Ochterski, R. L. Martin, K. Morokuma, V. G. Zakrzewski, G. A. Voth, P. Salvador, J. J. Dannenberg, S. Dapprich, A. D. Daniels, Ö. Farkas, J. B. Foresman, J. V. Ortiz, J. Cioslowski, D. J. Fox. Gaussian 09 Revision D.01, Gaussian Inc., Wallingford CT, 2013.
[99] CFOUR, Coupled-Cluster techniques for Computational Chemistry, a quantum-chemical program package by J. F. Stanton, J. Gauss, M. E. Harding, P. G. Szalay, with contributions from A. A. Auer, R. J. Bartlett, U. Benedikt, C. Berger, D. E. Bernholdt, Y. J. Bomble, L. Cheng, O. Christiansen, M. Heckert, O. Heun, C. Huber, T.-C. Jagau, D. Jonsson, J. Jus'elius, K. Klein, W. J. Lauderdale, D. A. Matthews, T. Metzroth, L. A. Mück, D. P. O'Neill, D. R. Price, E. Prochnow, C. Puzzarini, K. Ruud, F. Schiffmann, W. Schwalbach, S. Stopkowicz, A. Tajti, J. Va'zquez, F. Wang, J. D. Watts, and the integral packages MOLECULE (J. Almlöf, P. R. Taylor), PROPS (P. R. Taylor), ABACUS (T. Helgaker, H. J. A. Jensen, P. Jørgensen, J. Olsen), and ECP routines by A. V. Mitin, C. van Wüllen. For the current version, see http://www.cfour.de.
[100] A. Karton, E. Rabinovich, J. M. L. Martin, B. Ruscic, *J. Chem. Phys.* **2006**, *125*, 144108.
[101] A. Karton, J. M. L. Martin, *J. Chem. Phys.* **2012**, *136*, 124114.

Manuscript received: October 5, 2022
Revised manuscript received: December 12, 2022
Accepted manuscript online: December 12, 2022
Version of record online: January 3, 2023